

# Swelling of phospholipid floating bilayers: the effect of chain length

Giovanna Fragneto<sup>1\*</sup>, Thierry Charitat<sup>2</sup>, Edith Bellet-Amalric<sup>3</sup>, Robert Cubitt<sup>1</sup>, François Graner<sup>4</sup>

<sup>1</sup> *Institut Laue-Langevin, 6 rue Jules Horowitz, B.P. 156, 38042 Grenoble Cedex, France*

<sup>2</sup> *Institut Charles Sadron <sup>†</sup>, 6 rue Boussingault, F-67083 Strasbourg Cedex, France*

<sup>3</sup> *DRFMC/SP2M/SGX, CEA, 17 Av. des Martyrs 38054 Grenoble Cedex 9, France*

<sup>4</sup> *Spectrométrie Physique <sup>‡</sup>, B.P. 87, F-38402 St Martin d'Hères Cedex, France*

(January 9, 2022)

The equilibrium distance between two lipid bilayers stable in bulk water and in proximity of a substrate was investigated. Samples consisted of a homogeneous lipid bilayer, floating near an identical bilayer deposited on the hydrophilic surface of a silicon single crystal. Lipids were saturated di-acyl phosphocholines, with the number of carbon atoms per chain,  $n$ , varying from 16 to 20. The average and r.m.s. positions of the floating bilayer were determined by means of neutron specular reflectivity. Samples were prepared at room temperature (i.e. with the lipids in the gel phase) and measurements performed at various temperatures so that the whole region of transition from gel to fluid phase was explored. Data have been interpreted in terms of competition between the interbilayer potential and membrane fluctuations and used to estimate the bending rigidity of the bilayer.

87.16.Dg: Membranes, Bilayers and Vesicles.

87.15.Va: Fluctuations

61.12.Ha: Neutron reflectometry

68.15.+e: Liquid thin films

## I. INTRODUCTION

The basic building blocks of cell membranes are lipid bilayers. They provide mechanical stability and have a strong tendency to form closed structures. They support membrane proteins and have sufficient flexibility for vesicle budding and membrane fusion [1]. The physical properties of lipids are fundamental for understanding their biological functions. Because of their complexity, the duplication of cell membranes and the investigation of their interactions with peptides or proteins is difficult. An increasing need for biomimetic models has recently caused the revival of a classical approach: the use of lipid bilayers [2]. A considerable effort has led to numerous successes in preparing new types of samples and corresponding structural measurement techniques. These can resolve sub-nanometric details, leading to investigations of lipid-lipid, lipid-peptide or lipid-protein interaction mechanisms.

Phospholipids present a variety of different phases as a function of temperature [3]. Cooling from high to low temperature, lipids overcome the fluid to gel phase transition at a temperature commonly known as  $T_m$  (melting temperature). While in the fluid phase,  $L_\alpha$ , lipid chains are in a liquid-like conformation and mobile in the lateral direction, in the gel phase,  $L_\beta$ , chains are stiffer. For some lipids, just below  $T_m$ , there is the so-called ripple phase,  $P_\beta$ , where the lamellae are deformed by a periodic and static out of plane modulation. Biophysical studies of membrane-membrane and membrane-protein interactions require well controlled model systems [2,4]. In previous papers [5,6] a new model system has been described consisting of stable and reproducible double bilayers, in which a lipid bilayer floats at 2-3 nm on top of an adsorbed one. Since the second bilayer is only weakly bound, the preparation is delicate but results are reproducible. The process relies on three vertical Langmuir-Blodgett depositions, followed by a horizontal Langmuir-Schaeffer one; this method is efficient when lipids are in the gel phase and by raising the temperature the floating bilayer overcomes a phase transition becoming fluid and still stable.

The floating bilayer system has been very useful to probe bilayer-bilayer interactions, and is currently being improved to accommodate for charges in water and in the bilayer, so that lipid/peptide interactions can be studied in physiological buffers. Since it has the potential to support transmembrane proteins, this system can be a better biomimetic model membrane than supported single bilayers. Floating bilayers offer the following advantages: they are well-defined structures, where the composition of each leaflet of the bilayer can be chosen separately; they are immersed in aqueous solution and they allow information on a single bilayer to be obtained [7,8], contrarily to the

---

\*to whom correspondence should be addressed at fragneto@ill.fr

<sup>†</sup>CNRS - UPR 22, Université Louis Pasteur

<sup>‡</sup>CNRS - UMR 5588, Université Grenoble I

classical models of multilamellar vesicles or stacked systems. They are stable in the fluid phase and swelling of the water layer between the bilayers can be observed with this system around the phase transition.

A systematic study of the swelling is presented here, where the values of the distance of the floating bilayer from the adsorbed one were determined for phosphocholine lipids with saturated double chains and a number of carbon atoms,  $n$ , per chain from 16 to 20. For all samples a more or less broad region around the main phase transition temperature has been detected characterised by a swelling of the layer of water between the bilayers of about 1 nm. Giant swelling (i.e. swelling  $\gg$  1nm) was also observed with samples having 17 and 18 carbon chains. Results from a self-consistent theory [9], that has been developed to extract the values of the bending modulus of the membranes from the experimental data, will be shown.

## II. MATERIALS AND METHODS

Lipids were purchased from Avanti Polar Lipids (Lancaster, Alabama, USA) and used without further purification. They are phosphatidyl-cholines (PC) with different chain lengths (for simplicity they are indicated as Di- $C_n$ -PC): di-palmitoyl (Di- $C_{16}$ -PC), di-heptadecanoyl (Di- $C_{17}$ -PC), di-stearoyl (Di- $C_{18}$ -PC), di-nonadecanoyl (Di- $C_{19}$ -PC) and di-arachidoyl (Di- $C_{20}$ -PC). Fully deuterated (Di- $C_{18}$ -PC) (d83) was also used. Several attempts to prepare floating bilayers from fully deuterated Di- $C_{16}$ -PC failed. Hydrogenated lipids were measured in  $D_2O$  and fully deuterated lipids in  $H_2O$  and Silicon Match Water, (i.e. mixture of  $H_2O$  and  $D_2O$  with a scattering length density =  $2.07 \times 10^{-6} \text{ \AA}^{-2}$ ). The minimum and maximum temperatures investigated are: 25.0-82.6°C for  $n=16$ ; 25.0-55.6°C for  $n=17$ ; 25.0-64.1°C for  $n=18$ ; 25.0-60.8°C for  $n=19$  and 25.0-68.6°C for  $n=20$ .

Two kinds of silicon substrates were used: (i) of surface  $5 \times 5 \text{ cm}^2$  and 1 cm thick obtained and polished by SESO (Aix-en Provence, F) with a r.m.s. roughness 0.15 nm measured on  $300 \times 300 \mu\text{m}^2$ ; and (ii) of surface  $8 \times 5 \text{ cm}^2$  and 2 cm thick obtained from Siltronix (Archamps, F) and polished by the Optics Laboratory of the European Synchrotron Radiation Facility (Grenoble, F) with a technique including diamond powder treatment and producing high quality crystal surfaces with r.m.s. roughness of  $< 0.2 \text{ nm}$ .

The silicon blocks were made highly hydrophilic with a UV/ozone treatment as in [6]. Lipids were deposited on the substrate with a combination of the Langmuir-Blodgett and Langmuir-Schaeffer techniques as described in [5,6]. Depositions were done at room temperature, and the lipids compressed to surface pressures varying with the lipid chain length (40 mN/m for  $n=16,17,18$ ; 35 mN/m for  $n=19$  and 30 mN/m for  $n=20$ ). Transfer ratios for the first layers were always high and of the same order as samples described in [6]. They improved as the chain length increased and attained the value of 1.0 for  $n=18,19,20$ . It was found that the horizontality of the sample in the Schaeffer dip is crucial for a good quality sample. In fact, while in [5,6] during the Schaeffer dip the substrates were slightly inclined so that no air bubbles would form on the solid surface, here systematic measurements on Di- $C_{18}$ -PC samples were made and it was found that a sample surface as parallel as possible to the water surface (micrometric screws were used) prevents the formation of bubbles and gives transfer ratios always bigger than 0.97.

While it is difficult to prepare samples with short phospholipid chains (e.g. with DMPC), it has been found that this is possible if the first layer is chemically grafted to the surface [10], although in this case the coverage of the DMPC floating layer is not always optimal and reproducibility problems are encountered. This method when applied to longer chain lipids has resulted in the formation of very stable and defect-free layers (work in progress).

## III. NEUTRON REFLECTIVITY: BASIC PRINCIPLES AND MEASUREMENTS

Specular reflectivity,  $R(Q)$ , defined as the ratio between the specularly reflected and incoming intensities of a neutron beam, is measured as a function of the wave vector transfer,  $Q = 4\pi \sin \theta / \lambda$  perpendicular to the reflecting surface, where  $\theta$  is the angle and  $\lambda$  the wavelength of the incoming beam.  $R(Q)$  is related to the scattering length density across the interface,  $\rho(z)$ , and for values of  $Q$  bigger than the critical value for total reflection, it decays as  $Q^{-4}$  [11].

Specular reflectivity allows the determination of the structure of matter perpendicular to a surface or an interface. Experiments are performed in reflection at grazing incidence. Samples must be planar, very flat and with roughness as small as possible ( $< 0.5 \text{ nm}$ ). The data presented here were collected at the High Flux Reactor (HFR) of the Institut-Laue Langevin (ILL, Grenoble, F) both on the small angle diffractometer D16 and the high flux reflectometer D17. Instrument set-up and the data collection method on D16 have been described in [5]. A monochromatic neutron beam of wavelength  $\lambda = 4.52 \text{ \AA}$  impinged on the sample at grazing incidence. A two-dimensional  $^3\text{He}$  wire detector was kept in a fixed position covering the angular  $2\theta$  range  $0^\circ - 9^\circ$ . The beam was vertically focused at the detector position in order to gain intensity without worsening divergence. The dual mode instrument D17 [12,13] is designed

to take advantage of both Time-Of-Flight (TOF) and monochromatic methods of measuring reflectivity. In this study measurements were all taken with the instrument in the TOF mode by using a spread of wavelengths between 2 and 20 Å at two incoming angles (typically 0.7° and 4°) and with a time resolution, defined by two rotating choppers, of  $\Delta t/t = 1\%$  and 2-5%, respectively, where  $\Delta t$  is the neutron pulse duration. The beam was defined in the horizontal direction by a set of two slits, one just before the sample and one before a vertically focusing guide. Neutron reflectivity from the same sample was measured at different temperatures monitored with a thermocouple (equilibration time 25 minutes, stability  $< 0.1^\circ\text{C}$ , absolute precision  $< 0.3^\circ\text{C}$ ), in the water-regulated sample chamber already described in [5]. Two types of measurements were performed: (i) up to  $Q \sim 0.08 \text{ \AA}^{-1}$ ; (ii) over the whole available  $Q$ -range defined as follows.

For measurements done on D16, the whole available  $Q$ -range (0.003-0.22  $\text{\AA}^{-1}$ ) was scanned in eight hours, after equilibration. On D17 the useful  $Q$ -range, before hitting the sample background, spanned from 0.007 to 0.25  $\text{\AA}^{-1}$  and was measured in about two hours, also after equilibration. The equilibration time varied depending on the step of temperature increase or decrease. For a step of  $1^\circ\text{C}$  it was of about 15 minutes.

#### IV. DATA ANALYSIS: MODEL FITTING OF REFLECTIVITY DATA

A reflectivity curve essentially reflects the sample density perpendicular to the substrate surface, or rather the square modulus of its Fourier transform. Data analysis requires a good knowledge of the sample and here it was done via model fitting. Born and Wolf give a general solution, the so called optical matrix method [14], to calculate the reflectivity from any number of parallel, homogeneous layers, which is particularly useful since any layer structure can be approximately described by dividing it into an arbitrary number of layers parallel to the interface, each having a uniform scattering length density. In previous studies [6,15], multiple contrast neutron measurements at room temperature had allowed the determination within Å precision of the profile of adsorbed and floating bilayers. Each bilayer is resolved into outer-inner-outer slabs: outer slab = heads (phospho-choline and glycerol groups), inner slab = tails (hydrocarbon chains). A water film of thickness  $D_w$  separates the adsorbed and floating bilayers. Together with the natural oxide layer present on the silicon crystal and the hydration water layer between the substrate and the first lipid layer, this leads to 9 slabs in total, each one having its own average thickness and scattering length density. Each interface between two slabs has a certain width, also called r.m.s. roughness. Since this is included into the density profile, it can be determined by fits of reflectivity curves, but it is not possible to determine whether it is a static intrinsic width or an average over the neutron beam correlation length of temporal or spatial fluctuations.

The present work focuses on thicknesses and roughnesses only. By starting from the above 9-slab model, with the tabulated values of  $\rho$  (see Tables in refs. [5,6]) the relevant parameters to the data were fitted for all systems in the gel phase (the starting point of all measurements was the collection of the reflectivity profile at  $25^\circ\text{C}$ ). The first reflectivity minimum abscissa is very sensitive to the thickness of both water films. The second reflectivity minimum position is mainly sensitive to the thickness of the first bilayer tail slab; the amplitudes and sharpnesses of both minima depend upon bilayer roughness (see figures 1 and 2). All slabs were easily distinguished, except that the high hydration of lipid heads [16,17] prevents a localization of the heads/ $\text{D}_2\text{O}$  interface to better than 0.1 nm. Correcting the scattering length densities for temperature variations had no significant effect on the positions of the reflectivity minima, hence on the fitted parameters. For data at high temperatures the analysis concentrated on the exact determination of  $D_w$ . When giant swelling occurred, data analysis was complicated by the fact that the high values found for the roughness limit the usefulness of the analysis based on homogeneous layer models, leading to large error bars for  $D_w$  and  $\sigma$ .

In a parallel study (in progress) of specular and off-specular reflectivity from synchrotron radiation on similar samples the wider  $q$ -range attained and therefore the inadequacy of the box model fitting [18] has made it necessary to use the one Gaussian hybrid model described in [19]. The results as far as  $D_w$  is concerned are in perfect agreement with the values obtained from neutron reflectivity using the box model.

Figure 1 gives some examples of the collected data. The reflectivity curves obtained from hydrogenated lipids in the fluid phase at randomly chosen temperatures, as well as the best fits to the data, are shown. As expected the main differences are observed at the second minimum which is dependent on the single bilayer structure. Figure 2 is an example of curves collected for the system Di- $\text{C}_{17}$ -PC in the gel and fluid phases and in the transition region, as well as the best fits to the data. The density profiles obtained from the model that best fits the data are given in the insert.

## V. DATA ANALYSIS: CALCULATION OF BENDING MODULUS

The self-consistent theory described in [9] for a fluid bilayer floating near a solid substrate was applied to the results of this study. The basic principles are briefly described below. The shape of the substrate potential determines the amplitude  $\sigma$  of thermal fluctuations which itself determines the effective potential [3,20] felt by the bilayer. The average bilayer position and its r.m.s. fluctuation amplitude are thus coupled and depend both on temperature and bending energy of the membrane. This model situation is experimentally relevant as already reported in [4]. Three self-consistent equations may be written for the partition function,  $\mathcal{Z}$ , the equilibrium inter-bilayer distance,  $D_w$ , and the r.m.s. fluctuation amplitude,  $\sigma$ :

$$\begin{aligned}\mathcal{Z} &= \int dz e^{-16 \frac{\kappa}{(k_B T)^2} \sigma^2 U(z) - 3 \frac{(z - D_w)^2}{8\sigma^2}}, \\ D_w &= \frac{1}{\mathcal{Z}} \int dz z e^{-16 \frac{\kappa}{(k_B T)^2} \sigma^2 U(z) - 3 \frac{(z - D_w)^2}{8\sigma^2}}, \\ \sigma^2 &= \frac{1}{\mathcal{Z}} \int dz (z - D_w)^2 e^{-16 \frac{\kappa}{(k_B T)^2} \sigma^2 U(z) - 3 \frac{(z - D_w)^2}{8\sigma^2}}.\end{aligned}\tag{1}$$

where  $k_B$  is the Boltzmann constant,  $T$  the temperature and  $\kappa$  the bilayer bending rigidity modulus.  $U(z)$  is a one dimensional potential describing the interaction between the bilayer and the substrate.

At short distances, with  $z$  typically of the order of the hydration length  $z_0 \sim 0.6$  nm or smaller, the potential is dominated by the hydration repulsion due to water molecules inserted between hydrophilic lipid heads [3] :

$$U_h(z) = A_h \exp\left(-2 \frac{z}{z_0}\right).\tag{2}$$

At long distances, for a neutral membrane, the dominant term in  $U(z)$  is due to van der Waals attraction :

$$U_{vdW}(z) = -\frac{A}{12\pi} \left[ \frac{1}{z^2} - \frac{2}{(z + \delta)^2} + \frac{1}{(z + 2\delta)^2} \right],\tag{3}$$

where  $\delta$  is the bilayer thickness and  $A$  the Hamaker constant.

Here, it is assumed that  $A$  does not diverge and does not undergo any marked minimum so that its variations with temperature are negligible (compared to those of  $\kappa$ ) and therefore  $A$  is constant in what follows.

The dimensionless parameter  $\beta$  :

$$\beta = \frac{(k_B T)^2}{A\kappa},\tag{4}$$

determines the position and the fluctuations of the membrane. At low values of  $\beta$ , the bilayer is stiff, barely fluctuating in a strong minimum of potential energy. At high values of  $\beta$ , the bilayer is soft and has large fluctuations leading to the increase of the mean distance  $D_w$  to the adsorbed bilayer.

By eliminating  $\mathcal{Z}$  from the three self-consistent equations (1), two of the three physical quantities  $D$ ,  $\sigma$  and  $\beta$  can be expressed as a function of the third one. Experimentally,  $D_w$  and  $\sigma$  are measurable quantities while  $\beta$  is much more difficult to measure, especially for bilayers in the gel phase [21]. Therefore, measurements of  $D_w$  are used here to estimate  $\beta$  and  $\sigma$  by using a classical numerical resolution of equations (1) [9]. The validity of this approach is tested by comparing  $\sigma$  to the experimental data.

## VI. RESULTS AND DISCUSSION

The analysis of the reflectivity curves has led to the determination of the water layer  $D_w$  and the bilayer roughness  $\sigma$  (see section IV). The main results are summarised in Table I as well as in Figures 3 to 9. It was found that the silicon crystals were covered by a  $1.2 \pm 0.1$  nm thick oxide. A thin water film of thickness  $0.6 \pm 0.1$  nm separated it from the adsorbed bilayer. Both in the gel and in the fluid phases the thickness of the headgroups was  $0.8 \pm 0.1$  nm. The thickness of chains ( $D_{chain}$ ) in the gel phase (at 25°C) is reported in Table I for all lipid species. In the fluid phase those thicknesses were usually lower by about 0.2 nm. The bilayers were found to incorporate 5 to 10% of water. As for the roughness, well below and above the transition region it was the same as the substrate, i.e.  $0.3 \pm 0.1$  nm. In the transition region it increased (see below).

Figures 3 and 4 are a summary of the changes of  $D_w$  with temperature for all lipid species. Figure 3 refers to measurements from hydrogenated lipids in  $D_2O$  and Figure 4 refers to measurements of deuterated Di-C<sub>18</sub>-PC in  $H_2O$  and contrast match water. On the x-axis is  $T-T_m$ , i.e the difference between the temperature at which the measurement was taken and the value of the melting temperature (the values used for  $T_m$  are listed in Table I). For all lipids a very similar behaviour was observed, that is an increase of both  $D_w$  and  $\sigma$  in a certain range of temperature around the main phase transition (swelling region). The degree of swelling was always around 1 nm, and in two cases (n=17,18) giant swelling ( $\gg 1$  nm) was observed. The swelling temperature  $T_s$  defined as the temperature at which  $D_w$  and  $\sigma$  are maximum appears to be systematically 4 to 5 degrees below the melting temperature (see also figure 9). Above the transition, the floating bilayer is stable and  $D_w$  goes back to values similar to those found in the gel phase, although slightly higher. This equilibrium distance in the fluid phase increases slowly with temperature. In the gel phase, the minimum value  $D_{w,g}$ , listed in Table I, is obtained at the lowest measured temperature (i.e. 25°C). This value seems to be constant over a large temperature range, indicating that it is probably a good estimation of the bilayer position in the absence of thermal fluctuations. Figure 5 shows the variation of this minimum value with the lipid chain length n. At 25°C,  $D_{w,g}$  tends to decrease when n increases, and the effect seems to depend also on the oddness or evenness of n. It is unclear if this is fortuitous, to the best of the authors knowledge there are no other examples in the literature.

TABLE I. List of experimental data and literature parameters for the lipid species studied. n is the number of carbon atoms per chain in the formula Di-C<sub>n</sub>-PC;  $T_p$  is the temperature of transition from the gel to the ripple phase [22],  $T_m$  the temperature of main transition [22]. In column 4 are listed the regions of temperature where swelling was observed,  $T_s$  is temperature at which  $D_w$  reaches its maximum value  $D_w$  (max) and  $D_{w,g}$  is the value of  $D_w$  in Gel phase.  $D_{chain}$  is the chain region thickness, for the floating bilayer, in the gel phase (25°C).  $A_h$  and  $A$  are defined in the text and estimated from  $D_{w,g}$  (see below).

n	$T_p$ (°C)	$T_m$ (°C)	Swelling Region (°C)	$T_s$ (max) (°C)	$D_{chain}$ (nm)	$D_w$ (max) (nm)	$D_{w,g}$ (nm)	$\frac{A_h}{A}$
16	35-37	41-41.2 (41) <sup>2</sup>	(35-40)±1		3.2±0.2	3.3±0.2	2.2 ± 0.1	80 ± 15
17	43	48-49.8 (48) <sup>2</sup>	(40-45)±1	41.5±0.5	3.4±0.2	4.8±0.2	1.4 ± 0.1	23 ± 3
18	50-52	54.6-55 (55) <sup>2</sup>	(45-55)±1	51.5±0.5	3.6±0.2	6.0±0.4	1.8 ± 0.1	41 ± 7
18 (D) <sup>1</sup>		(50.5)	(37-50)±1		3.6±0.2	2.8±0.1	1.8 ± 0.1	41 ± 7
19	55.7-57.8	59-60 (60) <sup>2</sup>	(50-62)±1		3.8±0.2	2.3±0.1	1.2 ± 0.1	19 ± 2
20	62.1-63.7	63-66.4 (66) <sup>2</sup>	(56-64)±1		4.0±0.2	2.5±0.1	1.5 ± 0.1	26 ± 3

<sup>1</sup>Fully deuterated lipid; <sup>2</sup> Value given by Avanti polar Lipids and used for the figures;

The reproducibility of the observed effects was checked on different samples, from different experiments carried out in a period of two years on various silicon substrates and instruments (either D16 or D17). Figures 6(a) and 6(b) show results from samples with  $n=16$  and  $18$ . For clarity results have been split in different graphs so that the most notable effects could be highlighted. For the  $n=18$  case data from 4 samples are reported (samples A, B, C, and D in the caption). The temperature range where the swelling was observed is reproducible. The amplitude of swelling, that is the maximal distance reached, is variable from one sample to the other. In two cases giant swelling was observed, i.e. with lipids having  $n=17$  and  $n=18$ , the last one already described in [6]. It is not excluded that giant swelling occurs also with the other lipids investigated in this geometry. The limited available beam-time has not allowed exploring the transition temperature ranges in fine detail for all samples and since giant swelling is usually observed in narrow  $T$  ranges [23,24] it might have been missed in other cases.

The reversibility of the swelling was also studied. Figures 7(a) and 7(b) show results from one sample with  $n=17$  and two samples with  $n=18$  with data collected while heating up and cooling down once or twice, as indicated in the figure caption. The major result is that the swelling is reversible. On both figures, a weak increase in the maximum amplitude of the swelling with the successive heating and cooling processes is observed. It could still be due to the narrowness of the temperature range where swelling occurs, as mentioned above or it could be an indication that some defects of the bilayer like pinning points have been annealed. The swelling temperature is barely sensitive to cycles in temperature :  $T_s$  appears to be slightly lower when cooling down than when heating up. This could be related to the hysteresis of the main transition although the effect is too weak for a definitive interpretation.

Ref. [9] suggests a possible interpretation of the swelling in term of a balance between attraction by the substrate and entropic repulsion due to thermal fluctuation. The self-consistent theory briefly described in section V enables expressing  $D_w$  and  $\sigma$  as function of  $\beta$  by assuming that the dimensionless parameter  $\frac{A_h}{A}$  and the characteristic length  $z_0$  of the microscopic potential (equations 2 and 3) are known. Here it was assumed that  $z_0$  is equal to  $0.6 \text{ nm}$  and that it does not depend on chain length. By using the experimental value of  $D_w$  at low temperature ( $D_{w,g}$  in table I) and the microscopic potential, the ratio  $\frac{A_h}{A}$  was estimated for different values of  $n$  (Table I). From this approach, the experimental values of  $D_w$  are used to estimate  $\beta$  and the corresponding value of  $\sigma$  for each temperature. The value of  $\sigma$  is then compared to the r.m.s. roughness obtained by model fitting the data. Results from one representative example (i.e.  $n=16$ ) are given in figure 8. Agreement with all samples is remarkable (data not shown).

The derivation of an experimental estimation of  $\kappa$  implies the knowledge of the energy scale  $A$  (Hamaker constant). This value was estimated for all samples by normalising  $\kappa$  to the usual value  $10k_B T$  in the fluid phase. Values of  $A$  of the order of  $10^{-21} - 10^{-22} J$  were found in agreement with literature data [3]. This method forces the values for all different lipids to overlap artificially at high temperature. Figure 9 shows the value of the bending modulus calculated in that way. A minimum of the bending modulus is found around the main phase transition. Such minimum in  $\kappa$  is in agreement with literature data [25–28], even if its physical origin is unclear. It could be a signature of the proximity to a critical point in the phase diagram. As already mentioned, for Di-C<sub>18</sub>-PC in D<sub>2</sub>O the pre-transition temperature  $T_p = 51-52^\circ\text{C}$  [29,30] is close to the temperature at which the largest swelling is observed here. On the other hand, a minimum in  $\kappa$  is more likely to exist near the main (melting) transition  $T_m$  [27,31]. This would imply that for the floating bilayer  $T_m$  is lower than the value reported for multilamellar systems [29,30]. A comparable lowering of the melting temperature has been previously observed on single bilayers on a solid support [32] and was attributed to surface tension effects. Two experimental facts enforce this hypothesis: (i) the swelling temperature  $T_s$  seems to be always shifted by  $4-5^\circ\text{C}$  from the bulk  $T_m$  value (figure 3 and 9) independently of the phospholipid chain length; (ii) measurement made on deuterated Di-C<sub>18</sub>-PC in H<sub>2</sub>O in water exhibit also swelling and no literature data were found on a transition to the ripple phase for those deuterated species. In floating bilayers, a lateral stress might arise from possible pinning on defects. However, such a large tension would strongly limit the fluctuations and prevent both  $D_w$  and  $\sigma$  from increasing as much as we observe [33,34]. Finally, this interpretation can explain why the equilibrium distance is highly sensitive to small variations in the bending modulus and in the balance between attraction and repulsion (the samples are on the verge of unbinding) [33,35].

## VII. CONCLUSIONS AND PERSPECTIVES

Floating bilayers offer interesting advantages over other models for membranes. A structured bilayer, stable in time and free to fluctuate in the fluid phase enables in-situ studies of transmembrane channels or interactions between a lipid bilayer and membrane proteins. Its size, orientation, and the proximity of a smooth substrate enable reflectivity studies, and therefore structural characterisation in the fraction of nanometre scale. The composition of both lipids and surrounding medium can be varied with a certain freedom. Furthermore, this is a well defined geometry for comparison with theoretical models; it also provides different control parameters (temperature, composition of lipids

or water) to study the interaction between two membranes. Thanks to the excess water, a large increase in both the floating bilayer roughness and the inter-bilayer distance has been observed around  $T_m$  for a series of samples from phosphocholine lipids having different chain lengths. Anomalous swelling has been observed frequently at the main phase transition in multilamellar systems and it is object of debate [36,37] whether it is due to an increase of the bilayer thickness or to the swelling of the water layer between the membranes. The results presented here can help in this debate since the swelling that we observe is undoubtedly due to the increase in thickness of the water layer between the two bilayers. A parallel study is in progress for the determination of the fluctuation spectrum of the floating bilayers by using synchrotron radiation off-specular reflectivity measurements. In fact, while specular reflection gives information in the direction perpendicular to the interface, the lateral structure of the interface may be probed by the nonspecular scattering measured at reflection angles different from the specular one.

Since in that case the intensity of the reflected beam is much weaker than in the specular direction, the use of synchrotron radiation is necessary for obtaining a wide enough dynamic range for the analysis of these thin systems. Measurements have been performed both on double bilayers and on samples prepared by depositing three lipid layers on hydrophobically grafted silicon substrates. In this way the fluctuations of the layer closer to the substrate are reduced and information can be obtained only from the floating one. Results (to be published) indicate that the layer is under some tension (of the order of 3-5 mN/m) and such tension could explain why we observe the swelling at values of temperature lower than literature values of  $T_m$ .

Besides the bilayer fluctuation studies, the model is being improved to make it more relevant for interactions with biological systems. So far, we have succeeded inserting various amounts of cholesterol ranging from 0.5 to 10% cholesterol in the bilayers as well as negative charges (work in progress). The preparation of asymmetric bilayers, with the internal leaflet formed by phospho-ethanolamine headgroups and the outer one by phosphatidyl-choline headgroups is being optimised.

#### **Acknowledgments :**

The authors wish to thanks A. Freund and the staff of the Optics Laboratory at the ESRF for polishing the silicon crystals. We thank J. Daillant, A. Braslau (who was also present at one of the experiments), K. Mecke for useful discussions, J. Katsaras for suggesting the measurements at very high temperature, B.Stidder for help in sample preparation and J. Allibon for optimising the temperature control software that allowed for some sleep during the nights.

- 
- [1] Gennis, R. B. "Biomembranes, Molecular Structure and Function", Springer Verlag, New York, **1989**.
  - [2] Katsaras, Gutberlet, Eds. *Lipid Bilayers*, Springer, Biological Physics Series, **2000**.
  - [3] Lipowsky R., *Handbook of Biological Physics*, (R. Lipowsky and E. Sackmann editors), Elsevier **1995** Vol. 1, 521.
  - [4] Mouritsen, O.; Andersen, O. eds. *In search of a new biomembrane model*, Biologiske Skrifter 49, The royal danish academy of sciences and letters (Copenhagen) **1998**.
  - [5] Charitat, T.; Bellet-Amalric, E.; Fragneto, G.; Graner, F. *Eur. Phys. J. B* **1999**, 8, 583.
  - [6] Fragneto, G.; Charitat, T.; Graner, F.; Mecke, K.; Périno-Gallice, L.; Bellet-Amalric, E. *Europhys. Lett.* **2001**, 53, 100.
  - [7] Fragneto, G.; Bellet-amalric, E.; Graner, F. *Neutron and X-ray Studies of Lipid bilayers in Membrane Interacting Peptides and Proteins*, Editor F.Heitz, Research Signpost, India, **2002**.
  - [8] Leidy, C.; Kaasgaard, T.; Crowe, J. H.; Mouritsen, O.; Jørgensen, K. *Biophys. J.* **2002**, 83, 2625-2633.
  - [9] Mecke, K. R.; Charitat, T.; Graner, F. *Langmuir* **2003**, 19, 2080-2087.
  - [10] Hughes, A. V.; Goldar, A.; Gestenberg, M. C.; Roser, S. J.; Bradshaw, J. *J. Phys. Chem. Chem. Phys.* **53**, (2001) 100.
  - [11] Penfold, J.; Thomas, R. K. *J. Phys.-Cond. Matter* **1990**, 2, 1369.
  - [12] Cubitt, R.; Fragneto, G. *Neutron Reflection: Principles and Examples of Applications*, Chapter 2.8.3 of book "Scattering" edited by R. Pike and P. Sabatier, Academic Press, London, **2002**, pp 1198-1208
  - [13] Cubitt, R.; Fragneto, G. *Appl. Phys. A*, in press.
  - [14] Born, M.; Wolfe, E. *Principles Optics*; Pergamon Press: Oxford, U.K., **1989**.
  - [15] Fragneto, G.; Graner, F.; Charitat, T.; Dubos, P.; Bellet-Amalric, E. *Langmuir* **2000**, 16, 4581.
  - [16] Jendriasak, G.; Hasty, J. *Biochim. Biophys. Acta.* **1974**, 79, 337.
  - [17] Sun, W.J.; Sutter, R.M.; Knewtson, M.A.; Worthington, C.R.; Tristram-Nagle, S.; Zhang, R.; Nagle, J.F. *Phys. Rev. E* **1994**, 49, 4665.
  - [18] Shalke, ; Losche, M.; *Adv. Coll. Int. Sci.* **2000**, 88, 243.
  - [19] Nagle, J. F.; Zhang, R.; Tristram-Nagle, S.; Sun, W.; Petrache, H. I.; Suter, R. M.; *Biophys. J.* **1996**, 70, 1419.
  - [20] Helfrich, W.; *Z. Naturforsch.*, **1978**, 30a. 305-315.
  - [21] Koenig, S.; Pfeiffer, W.; Bayerl, T.; Richter, D.; Sackmann, E. *J. Phys. 2 (France)*, **1992**, 1589-1615.
  - [22] <http://www.lipidat.chemistry .ohio-state.edu/>
  - [23] Heimburg T.; *Biophys. J.* **2000**, 78, 1154-1165.
  - [24] Pabst, G.; Katsaras, J.; Raghunathan, V. A.; Rappolt, M.; *Langmuir* **2003**, 19, 1716.
  - [25] Méléard, P.; Gerbaud, C.; Pott, T.; Fernandes-Puente, L.; Bivas, I.; Mitov, M.; Dufourcq, J.; Bothorel, P. *Biophys. J.* **1997**, 72, 2616.
  - [26] Mishima, K.; Nakamae, S.; Ohshima, H.; Kondo, T. *Chem. and Phys. of Lipids* **2001**, 110, 27.
  - [27] Dimova, R.; Pouligny, B.; Dietrich, C. *Biophys. J.* **2000**, 9, 340.
  - [28] Lee, C.-H.; Lin, W.-C.; Wang J. *Phys. Rev. E* **2001**, 64, 020901.
  - [29] Guard-Friar, D.; Chen, C. H.; Engle, A. S. *J. Phys. Chem.* **1985**, 89, 1810.
  - [30] Okhi, K. *Biochem. Biophys. Res. Commun.* **1991**, 174, 102.
  - [31] Lemmich, J.; Mortensen, K.; Ipsen, J. H.; Hønger, T.; Bauer, R.; Mouritsen, O.G.; *Phys. Rev. E* **1996**, 53, 5169.
  - [32] Naumann, C.; Brumm, T.; Bayerl, T. M. *Biophys. J.* **1992**, 63, 1314.
  - [33] Lipowsky, R.; Leibler, S. *Phys. Rev. Lett.* **1986**, 56, 2541.
  - [34] Perino-Gallice, L.; Fragneto, G.; Mennicke, U.; Salditt, T.; Rieutord, F.; *Eur. Phys. J. E* **2002**, 8, 275.
  - [35] Leibler, S.; Lipowsky, R. *Phys. Rev. B* **1987**, 35, 7004.
  - [36] Lemmich, J.; Mortensen, K.; Ipsen, J.H.; Hønger, T.; Bauer, R.; Mouritsen, O.G.; *Phys. Rev. Lett.* **1995**, 75, 3958.
  - [37] Nagle, J. F.; Petrache, H. I.; Gouliarov, N.; Tristram-Nagle, S.; Liu, Y.; Suter, R. M.; Gawrisch, K.; *Phys. Rev. E* **1998**, 58, 7769.



## VIII. FIGURE CAPTIONS

FIG. 1. Reflectivity data (points) and best fits to the data (continuous lines) from all lipid species, Di-C<sub>n</sub>-PC, in the hydrogenated form and measured in D<sub>2</sub>O, in the fluid phase: (●) n=16 at T=44.2°C, (○) n=17 at T=45.8°C, (■) n=18 at T=55.4°C, (□) n=19 at T=58.9°C, (◇) n=20 at T=68.6°C.

FIG. 2. Reflectivity profiles (points) and best fits to the data (continuous lines) profiles for a double bilayer of Di-C<sub>17</sub>-PC at (●) T=25.0°C, (○) T=43.0°C and (□) T=45.8°C. In the insert are the scattering length density profiles as from the model used to fit the data: continuous thin line for T=25.0°C, continuous thick line for T=43.0°C and dashed line for T=45.8°C

FIG. 3. Distance,  $D_w$ , between the two bilayers from measurements from hydrogenated lipids vs. the deviation of temperature from the melting temperature,  $T-T_m$ ; (●) n=16; (○) n=17; (■) n=18; (□) n=19; (◇) n=20. Lines between points are added for clarity. Samples with n=16 and 18 were measured on D16; samples with n=17, 19 and 20 were measured on D17.

FIG. 4. Distance,  $D_w$ , between the two bilayers from measurements from deuteriated Di-C<sub>18</sub>-PC in Silicon Match Water (○) and H<sub>2</sub>O (△) and for hydrogenated Di-C<sub>18</sub>-PC in D<sub>2</sub>O (■) (same datas as figure 3) vs. the deviation of temperature from the melting temperature,  $T-T_m$ .

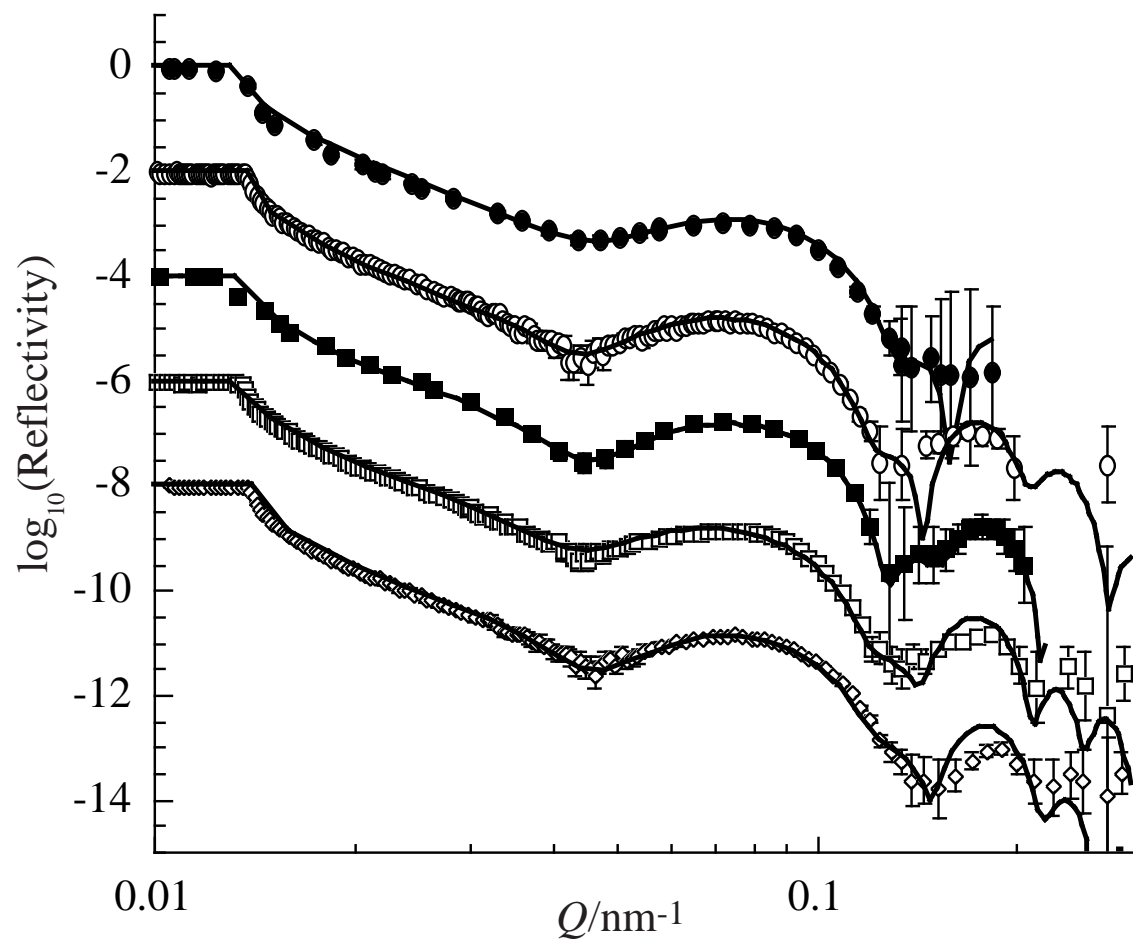
FIG. 5. Variation of  $D_w$  as a function of n at T=25°C.

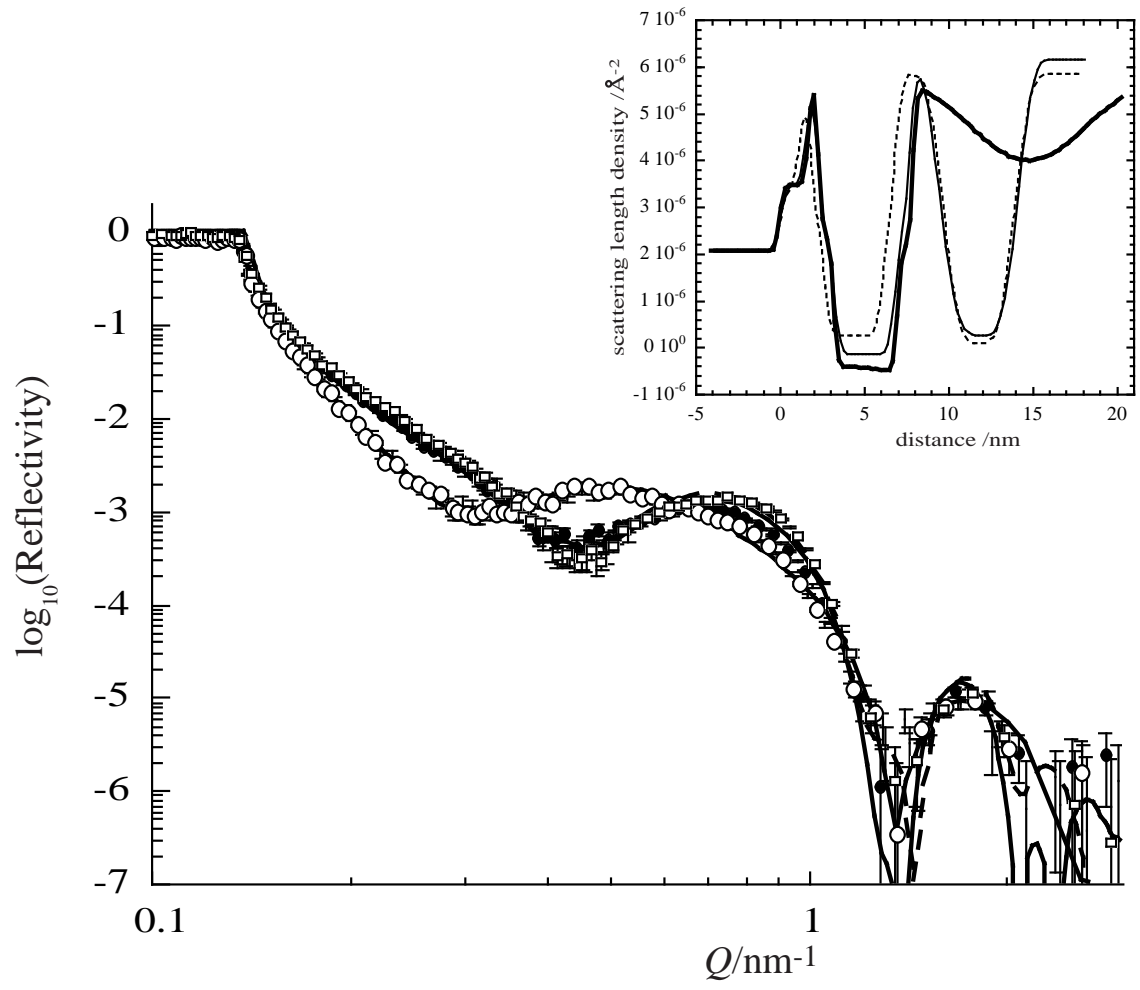
FIG. 6. (a) Distance,  $D_w$ , between two Di-C<sub>16</sub>-PC bilayers as a function of temperature, T. Experiments performed at different times on surfaces of different size: (○) 5x5 cm<sup>2</sup> (●) 5x8cm<sup>2</sup>. Both experiments were performed on D16.(b) Distance,  $D_w$ , between two Di-C<sub>18</sub>-PC bilayers. Experiments performed at different times over two years on different instruments: (□) sample A, measured on D17; (▽) sample A, second time raised in temperature after cooling from 58°C; (○) sample B, measured on D16; (△) sample C measured on D16; (◇) sample D measured on D16 [6].

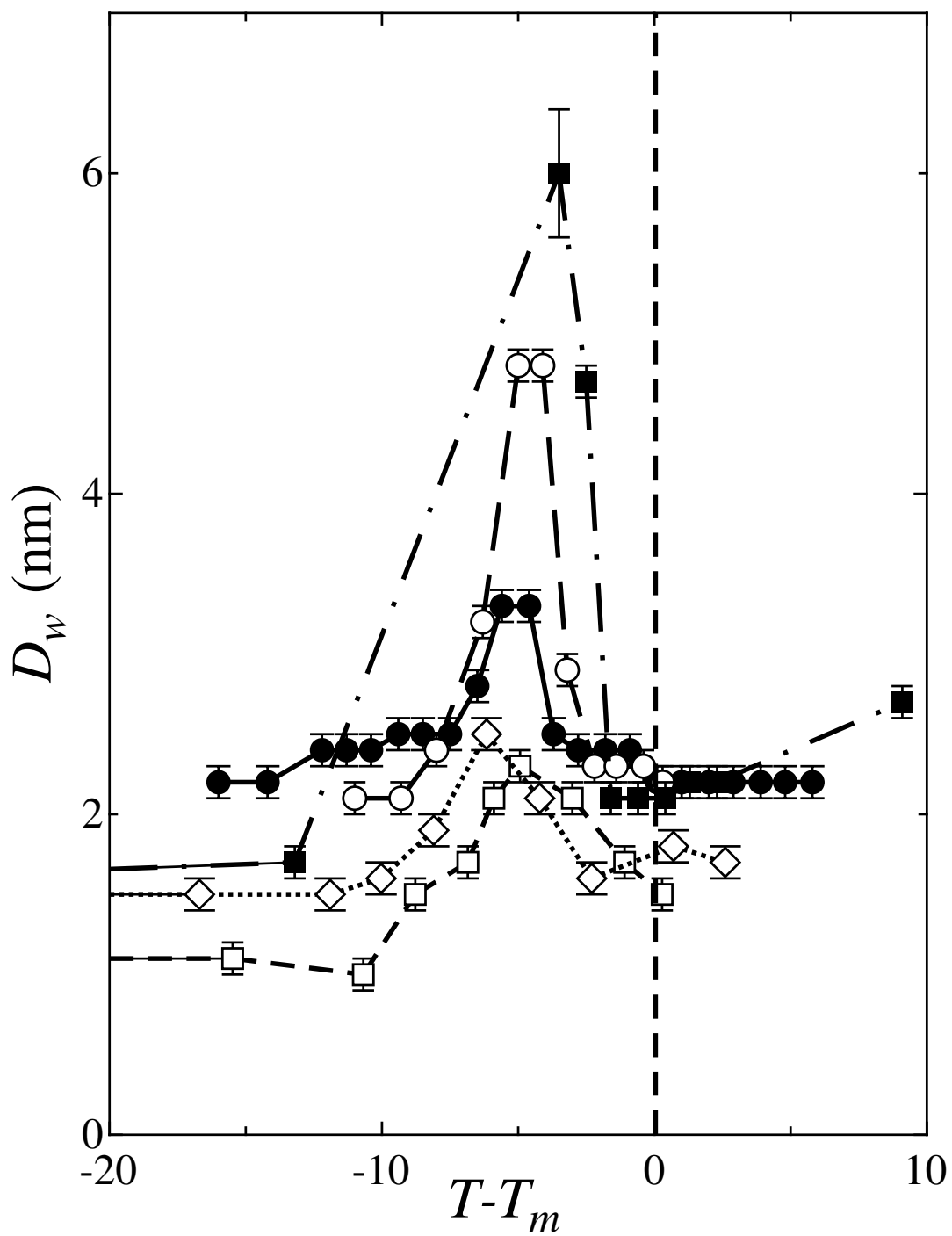
FIG. 7. (a) Distance,  $D_w$ , between two Di-C<sub>17</sub>-PC bilayers as a function of the temperature, T: (□) first time up in T; (●) first time down in T; (◇) second time up in T. (b) Distance,  $D_w$ , between two Di-C<sub>18</sub>-PC bilayers for 2 samples. Sample 1: (□) first time up (1); (■) first time down (2); (◇) second time up (3); Sample 2: (○) first time up (1'); (●) first time down (2'). All experiments were performed on D17.

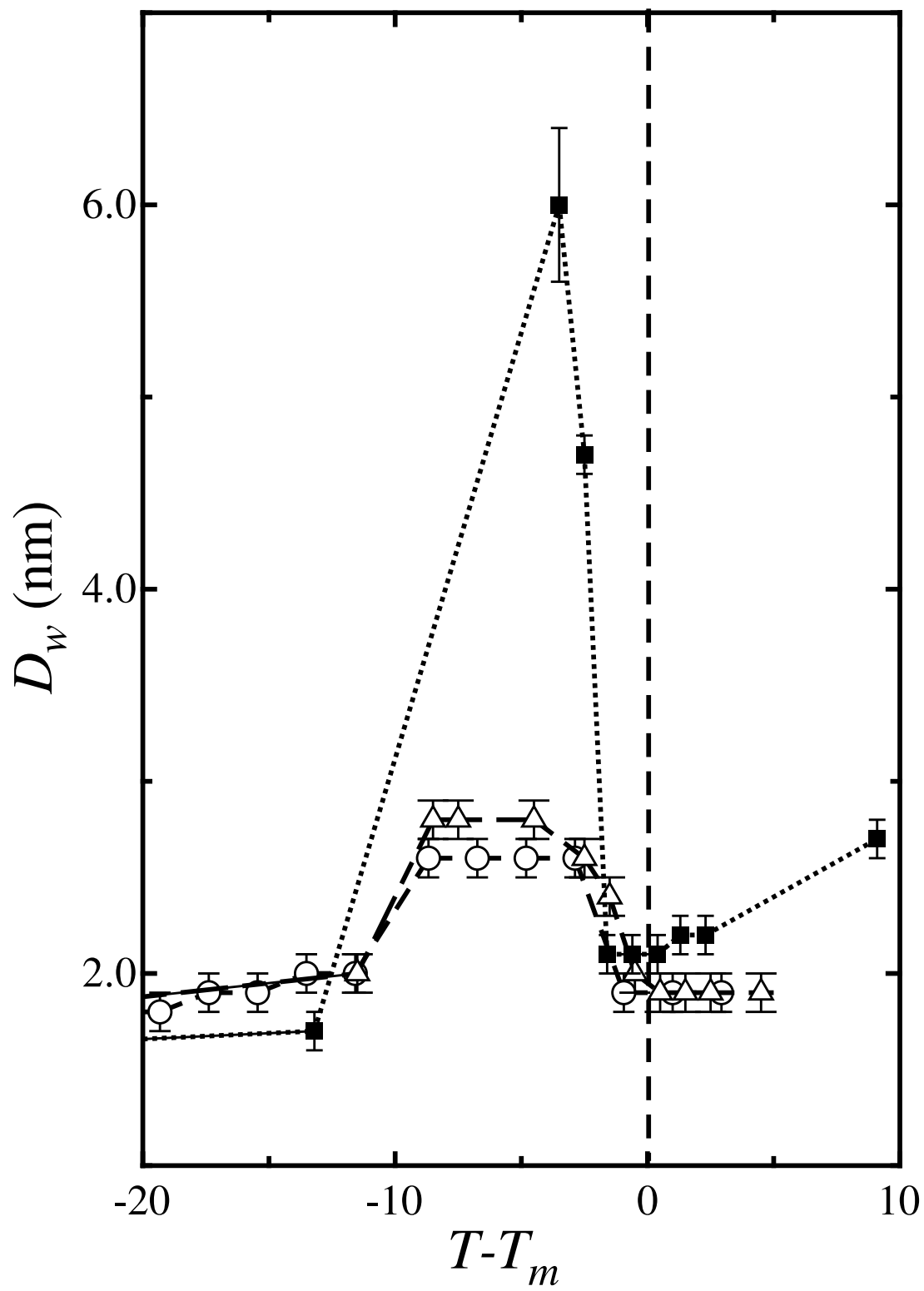
FIG. 8. Comparison of values of the r.m.s. roughness for a Di-C<sub>16</sub>-PC sample heated from 25 to 82.5°C as a function of temperature, T (□) as determined experimentally by model fitting the data and (●) as extracted with the self-consistent theory [9].

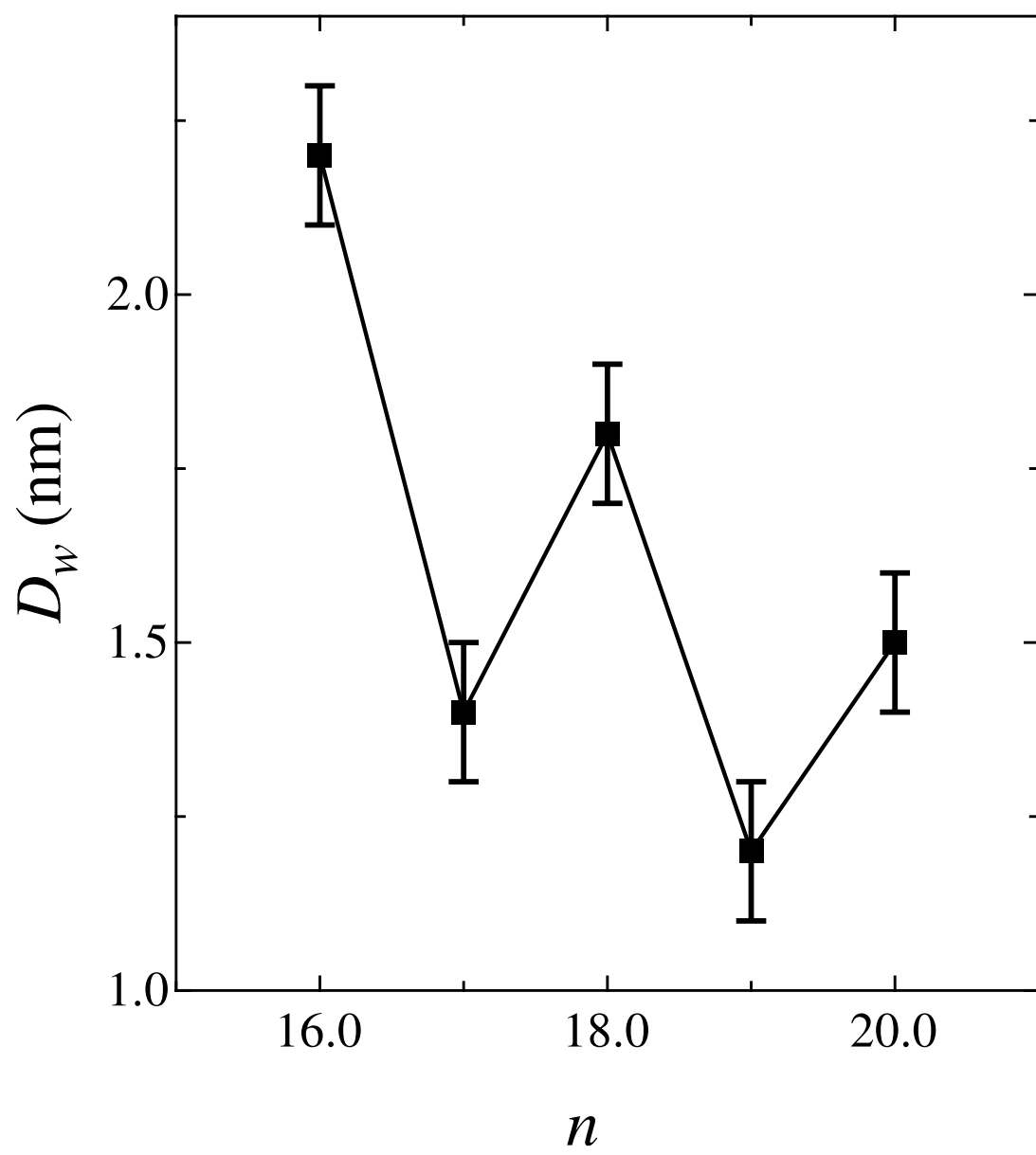
FIG. 9. Values of the bending modulus  $\kappa$  normalised by  $k_B T$  as a function of the deviation of temperature from the melting temperature,  $T-T_m$  for the samples Di-C<sub>n</sub>-PC with (●) n=16; (○) n=17; (■) n=18; (□) n=19; (◇) n=20. Values of  $\kappa$  are normalised to the arbitrary value  $10k_B T$  in the fluid phase. This method forces the values for all different lipids to overlap artificially in the fluid phase. The dashed line represents the pretransition temperature  $T_p$ .



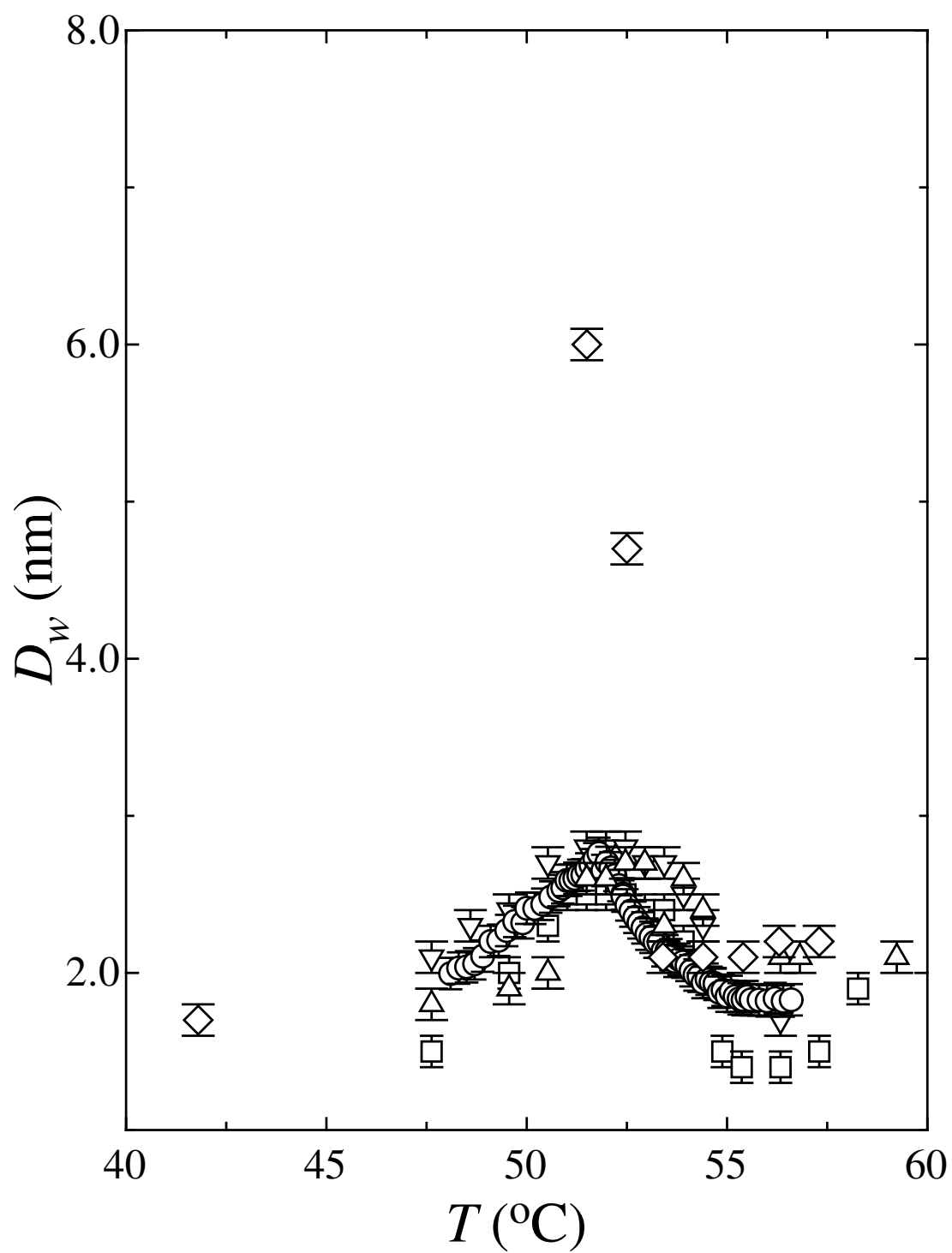






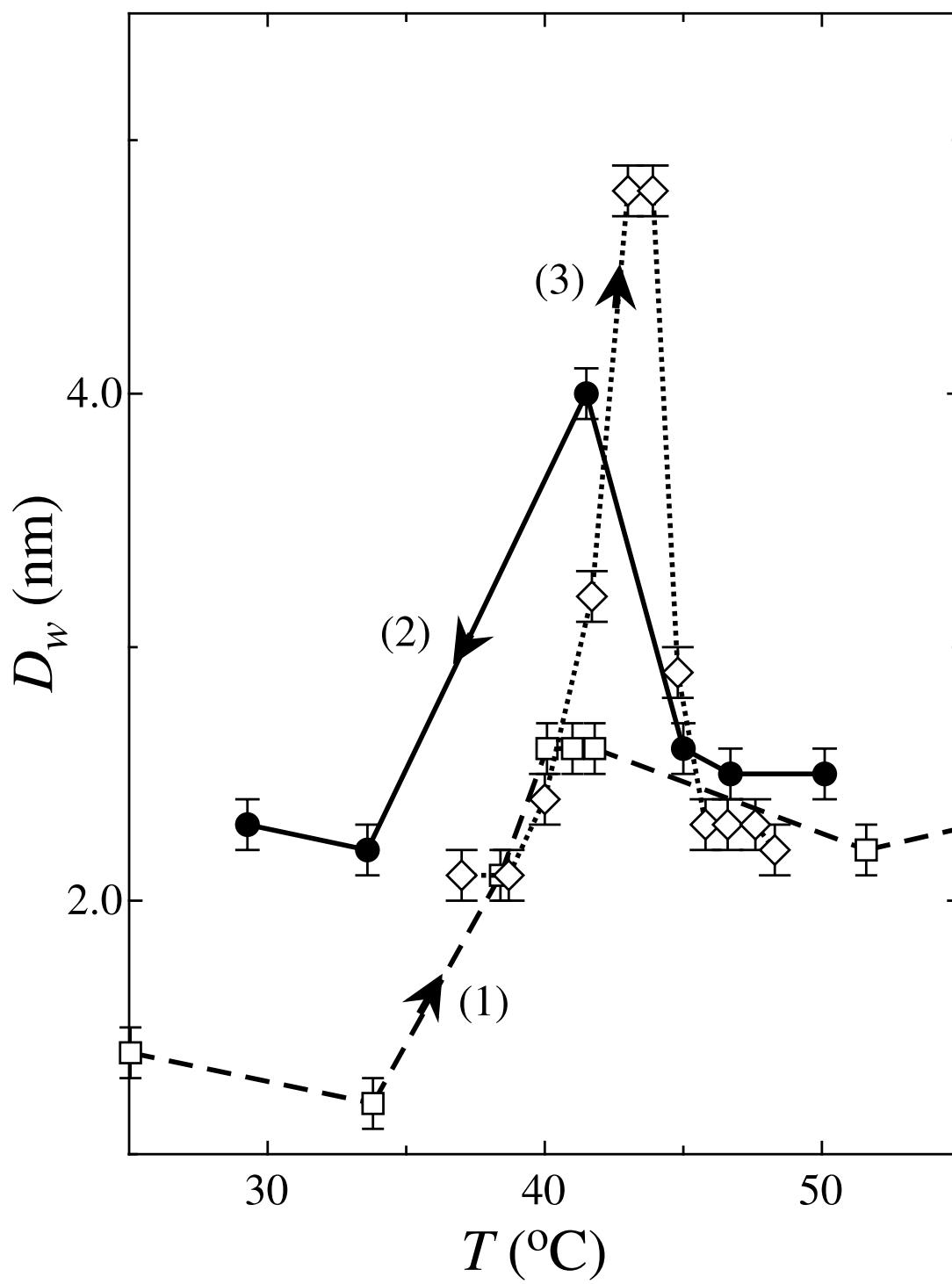






(b)





(a)

